

FIG. 1. Absorption coefficient for a majority group of electrons undergoing cyclotron resonance.

from the majority and much smaller total conductivity, one finds a new phenomenon: the minority electrons appear to be “screened” from strong interaction with the electromagnetic field and they will actually show a true resonance. However, under the conditions in which cyclotron resonance is observable the complex conductivity of the main group of electrons may have any phase angle. This leads to the possibility of many different line shapes for the absorption of the “screened” electrons, from a pure absorption to a pure dispersion curve. The shape depends upon where the subsidiary resonance is on the curve of Fig. 1. It should be noted that in any case there will be on the average a *reduction* in absorption coefficient due to the minority groups of electrons. Perhaps the most likely shape for these resonances is the usual line shape in metals as described by other authors.<sup>3</sup>

In the second experimental setup, the  $H$ -field is parallel to the sample cavity wall and one might as well use linear polarization. This we call the “longitudinal” case. Here the depolarizing effects completely eliminate the resonance of the majority group of electrons. However, the screening phenomenon can still take place, and a small group of electrons, if present, can show resonant absorption.

Results similar to Eq. (3) have recently been obtained elsewhere,<sup>4</sup> but the authors seemed to doubt their correctness on the basis that any depolarizing effect, if present, would appear capable of changing the result seriously. This point can be disposed of by noting how wall losses in wave-guide systems are normally calculated. That is, one usually assumes perfectly conducting walls in order to obtain the field distribution in the cavity, from which the wall currents are then obtained. This distribution can obviously contain no depolarizing fields ( $\nabla \cdot \mathbf{E} = 0$  everywhere). Then the finite surface impedance of the walls is introduced, assuming however that it does not appreciably perturb the field distribution, in order to compute the losses from the known currents. We feel that if the misgivings of reference 3 were sound, no calculation of cavity losses

would ever have been correct. This argument, however, does not apply in the “longitudinal” case, since there currents must flow into the surface, building up space charge within the metal, which is virtually impossible.

We have also investigated approximately the limitation on the sharpness of the cyclotron resonance produced by diffusion of electrons through the skin depth. We find that the rough relationship

$$Q^2 < \frac{1}{3} (H^2/8\pi)/nE_F \quad (4)$$

holds: i.e., the square of the maximum possible  $Q$  is given by the ratio of magnetic field to electron kinetic energy. This ratio is probably favorable for Bi and similar poor metals,<sup>2</sup> giving  $Q$ 's of 1–10, but will be fairly bad for normal metals except at high fields and frequencies.

*Note added in proof.*—F. J. Dyson has kindly called my attention to an article by M. Ia. Azbel' and M. I. Kaganov [Doklady Akad. Nauk. **95**, 41 (1954)] in which Eq. (3) is derived and the basis for a vigorous treatment of diffusion (anomalous skin effect) is laid.

<sup>1</sup> Galt, Yager, Merritt, Cetlin, and Dail, preceding Letter [Phys. Rev. **100**, 748 (1955)].

<sup>2</sup> D. Shoenberg, Trans. Roy. Soc. (London) **245**, 1 (1952).

<sup>3</sup> N. Bloembergen, J. Appl. Phys. **23**, 1383 (1952).

<sup>4</sup> Dresselhaus, Kip, and Kittel, Phys. Rev. **100**, 618 (1955).

## Ferrimagnetic Resonance in Single Crystals of Manganese Ferrite

J. F. DILLON, JR., S. GESCHWIND, AND V. JACCARINO  
Bell Telephone Laboratories, Murray Hill, New Jersey

(Received August 29, 1955)

FERRIMAGNETIC resonance has been studied in single crystals of manganese ferrite over a range of frequencies and temperatures. A quantitative analysis of the material for anions leads to the formula  $Mn_{0.98}Fe_{1.86}O_4$ .<sup>1</sup> Two types of transmission cavities

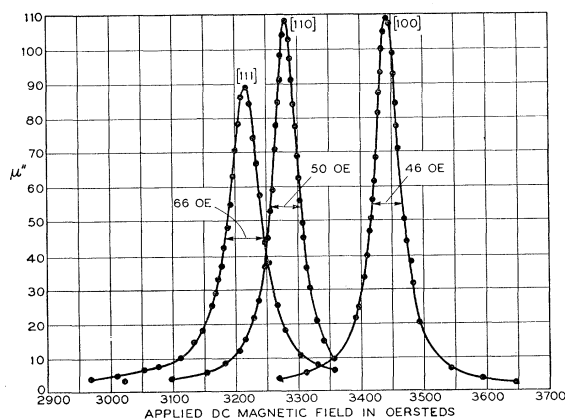


FIG. 1. Ferrimagnetic resonance line shapes measured with the dc magnetic field along the principal crystallographic directions. Measurements were made on a 0.0105-in. sphere at 9.3 kMc/sec, at room temperature.

were used; a high  $Q$  cylindrical cavity operating in the  $TE_{012}$  mode and a rectangular cavity in the  $TE_{102}$  mode. Oriented single crystal spheres of the ferrite were mounted on polystyrene rods and placed in the cavity at a position of maximum rf magnetic field which was perpendicular to the dc magnetic field. The dc magnetic field always lay in the (110) plane as the rod was rotated about its axis. The samples used were highly polished and were 0.0105 in. in diameter for 5.9 and 9.3 kMc/sec, and 0.0043 in. in diameter for the 24-kMc/sec experiments. The spheres were chosen this small to avoid dimensional resonances which result from the large value of  $\mu'$  in the vicinity of resonance. Dimensional resonances were observed in a 0.014-in. sphere at X-band at room temperature such that the line width was increased 15% relative to the 0.0105-in. sphere. On the other hand, a 0.0043-in. sphere gave the same line width as the 0.0105-in. sphere within the experimental error.

*Line Widths.*—As the magnetic field was varied through the resonance absorption, thereby lowering the transmission through the cavity, a precision calibrated attenuator placed between the output arm of the cavity and the microwave detecting crystal was adjusted to keep the power incident on the detector at a constant

TABLE I. Anisotropy constants and  $g$ -value at several temperatures as measured on 0.0105-in. sphere at 9.3 kMc/sec. The errors in the derived quantities were estimated on the basis of reproducibility of the measurements. The values of  $K_1/M_s$  and  $K_2/M_s$  coupled with  $M_s$  as measured by M. A. Gillo of this laboratory ( $M_s=351$  and 493 cgs units at 300° and 77°K respectively) can be used to calculate  $K_1$  and  $K_2$ .

	$K_1/M_s$	$K_2/M_s$	$g$
300 °K	$-79 \pm 3$	$6 \pm 10$	$2.004 \pm 0.002$
77 °K	$-412 \pm 5$	$-5 \pm 20$	$2.019 \pm 0.003$
4.2°K	$-433 \pm 15$	$-200$	2.060

level. Using the measured loaded  $Q$  of the cavity off resonance, the  $\mu''$  was then derived from the attenuator readings, thus making it independent of crystal detector characteristics. Figure 1 shows a plot of  $\mu''$  versus applied field at room temperature at 9.3 kMc/sec with the applied field along each of the three different symmetry directions. Line widths of 66, 50, and 46 oersteds were measured for the [111], [110], and [100] directions respectively. It is interesting to note that preliminary measurements at K-band indicate the line widths are the same, or perhaps smaller. These appear to be the narrowest ferrimagnetic resonance lines reported to date. The lines are closely Lorentz shaped over the measured region. The line width as a function of temperature in the easy direction ([111] axis) at 9.3 kMc/sec is shown in Fig. 2.

*First- and Second-Order Anisotropy Constants  $K_1/M_s$  and  $K_2/M_s$ .*—By measuring the dc field required for resonance at different orientations with respect to the crystal axes the anisotropy constants can be deter-

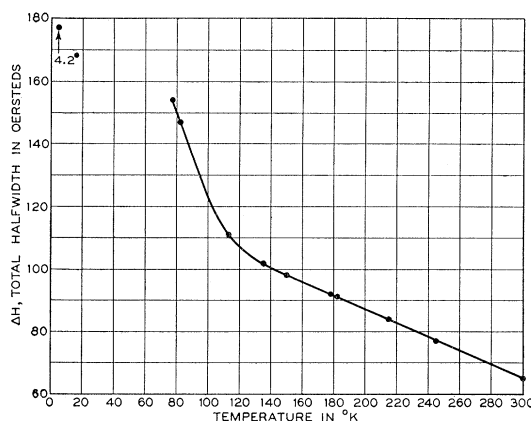


FIG. 2. Line width vs absolute temperature with the dc magnetic field along the easy direction ([111] axis). The line width is defined as the field interval between points of  $\frac{1}{2}\mu_{\max}''$ .

mined as well as the  $g$ -value.<sup>2</sup> The temperature dependence of the anisotropy constant  $K_1/M_m$  is plotted in Fig. 3, showing an increase with decreasing temperature. The most complete temperature data to date have been taken in the region of 9.3 kMc/sec. It will be noted that room temperature points at other frequencies lie on this curve, indicating the constancy of anisotropy energy as a function of frequency.<sup>3</sup> The value of  $K_2/M_s$  is considerably smaller than that of  $K_1/M_s$ , and moreover is smaller than the error in its determination from 300°K down to 77°K, as indicated in Table I. It should be noted though, that at 4.2°K  $K_2/M_s$  is strikingly large.

*The  $g$ -value.*—Room temperature measurements at 5.9, 9.3, and 24 kMc/sec indicate that the  $g$ -value is independent of frequency, its value being  $2.004 \pm 0.002$ . However, at 9.3 kMc/sec measurements were made over a range of temperatures and reveal a dependence, the  $g$ -value monotonically increasing with decreasing temperature reaching a value of  $2.019 \pm 0.003$  at 77°K. In view of the large  $K_2/M_s$  mentioned above at liquid helium temperatures, caution must be exercised in interpreting the  $g$ -value (see Table I) as well as the anisotropy constants at 4.2°K as obtained from the

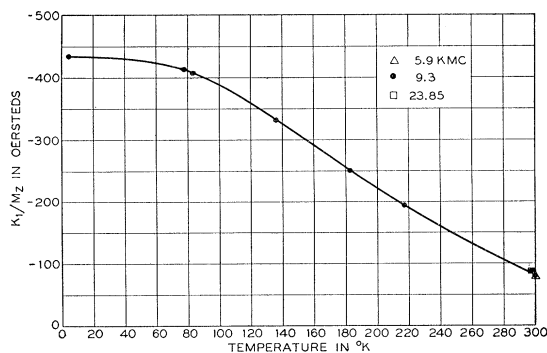


FIG. 3. Temperature variation of the first-order anisotropy constant  $K_1/M_s$ .

relations given in reference 2. A  $g$ -value so close to the free-electron  $g$ -value indicates a primarily spin-only magnetism (corresponding to a  ${}^6S_{5/2}$  ground state of  $Mn^{++}$ ).

We wish to thank Mr. J. White for his help in taking the measurements and we also wish to acknowledge helpful discussions with A. M. Clogston, H. Suhl, and L. R. Walker.

<sup>1</sup>The crystals used were obtained through Dr. G. W. Clark and Dr. R. W. Keblor of the Linde Air Products Company. Their dc resistivity was  $10^4$  ohm cm at  $300^\circ K$ . X-ray diffraction studies showed a lattice constant of 8.52 Å, and it was possible to account for every line with a spinel structure.

<sup>2</sup>The dc magnetic fields  $H_1$ ,  $H_2$ , and  $H_3$  required for resonance at a given frequency when applied along [100], [110], and [111] directions respectively are given by

$$H_{\text{eff}}^2 = \left( H_1 + \frac{2K_1}{M_s} \right)^2,$$

$$H_{\text{eff}}^2 = \left( H_2 - \frac{2K_1}{M_s} \right) \left( H_2 + \frac{K_1}{M_s} + \frac{1}{2} \frac{K_2}{M_s} \right),$$

$$H_{\text{eff}}^2 = \left( H_3 - \frac{4}{3} \frac{K_1}{M_s} - \frac{4}{9} \frac{K_2}{M_s} \right)^2,$$

where  $h\nu = g\beta H_{\text{eff}}$ . See, for example, L. R. Bickford, Jr., Phys. Rev. **78**, 449 (1950); Yager, Galt, Merritt, and Wood, Phys. Rev. **80**, 774 (1950).

<sup>3</sup>This result also agrees with the torque measurements of the anisotropy constant  $K_1$  of R. M. Bozorth *et al.* [Bozorth, Cetlin, Galt, Merritt, and Yager, Phys. Rev. **99**, 1898 (1955)].

## Double-Frequency Magnetic Resonance in a Free Radical\*

J. H. BURGESS AND R. E. NORBERG

Department of Physics, Washington University, St. Louis, Missouri  
(Received July 11, 1955)

AN unusual distortion of the absorption line shape has been observed in the course of double resonance experiments on hyperfine components resolvable in aqueous solutions of the free radical ion peroxyamine disulfonate,  $ON(SO_3)_2^{--}$ . The experiments involve the application of intense rf radiation near resonance for

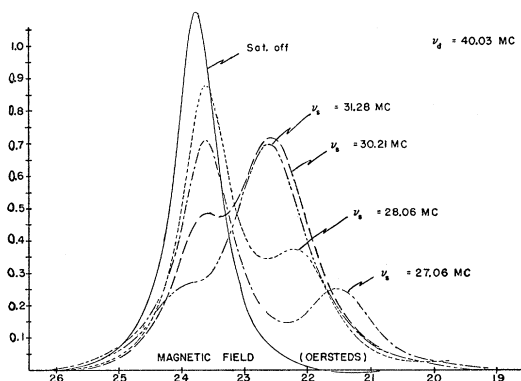


FIG. 1. Experimental absorption of the 3-4 transition (in notation of reference 1) plotted vs magnetic field for various frequencies of the second rf field, which saturates the 4-5 transition. The low-amplitude detecting frequency is fixed at 40.03 Mc/sec. The saturating rf field amplitude is of the order of 2 oersteds.

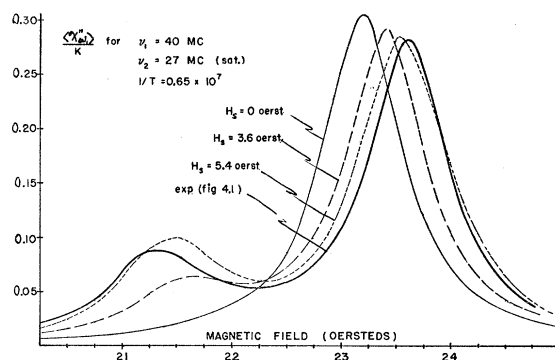


FIG. 2. Plots of Eq. 1 for three values of saturating field amplitude.  $\nu_d = 40$  Mc/sec and  $\nu_s = 27$  Mc/sec corresponding to one of the experimental curves of Fig. 1 which is the heavy curve superimposed here. The quantity  $T$  in Eq. (1) is determined from the experimental width of the unsaturated absorption curve.

one transition of the system, while detecting the resonance absorption of a second transition at low rf level.

If the two transitions share a common energy level, considerations of level population and lifetime predict a broadening and enhancement of the detected line as the first transition becomes saturated. However, in certain cases a "bump" is observed (see Fig. 1) on the absorption curve, at a position dependent both on the intensity of the saturating field and on the two applied frequencies.<sup>1</sup> The position of the bump corresponds qualitatively to the condition  $\nu_s + \nu_d = \nu_{ab} + \nu_{bc} = \nu_{ac}$ .  $\nu_s$ , the saturating frequency, is near resonance with the transition frequency  $\nu_{bc}$ , while  $\nu_d$ , the detecting frequency, is near resonance with the transition frequency  $\nu_{ab}$ . The experiments show that the effective gyromagnetic ratio of the combined transition,  $\gamma_{\text{eff}} = d\omega_{ac}/dH$ , determines the direction of the shift of the position of the bump. Increasing the amplitude of the saturating field, with frequencies  $\nu_s$  and  $\nu_d$  fixed, increases both the magnitude of the shift of the bump and the enhancement of the detected transition. In cases where  $\gamma_{\text{eff}}$  is small, the detected line is found to be broadened without observable structure.

An analysis based on the density matrix equation  $d\rho/dt = (1/i\hbar)[\mathcal{H}, \rho] - (1/T)(\rho - \rho_{\text{inst}})$ , where  $\rho_{\text{inst}}$  is the normalized Boltzmann factor appropriate to the instantaneous total energy of the system and  $T$  is the thermal relaxation time, leads to the following expression for  $\chi''(\omega_d)$ , the imaginary component of the susceptibility at the detecting frequency:

$$\chi''(\omega_d) = \frac{k}{D} \left[ \frac{\omega_d}{\omega_{ab}} [(x+y)^2 T^2 + 1] - F^2 \left( \frac{(x+y)}{\omega_{ab}} - 1 \right) \right]$$

$$+ \frac{k}{D} \frac{RF^2}{1 + y^2 T^2 + 4F^2} \left[ -(2x+y) \left( yT^2 + \frac{1+4F^2}{\omega_{bc}} \right) \right.$$

$$\left. + (x+2y)(x+y)T^2 + 3(1+F^2) \frac{\omega_s}{\omega_{bc}} \right], \quad (1)$$